Am. J. Hum. Genet. 77:1061–1074, 2005

The Role of Mannosylated Enzyme and the Mannose Receptor in Enzyme Replacement Therapy

Hong Du,[1] Mark Levine,[3] Chandrashekar Ganesa,[3] David P. Witte,[2] Edward S. Cole,[3] and Gregory A. Grabowski[1]

[1]Division and Program in Human Genetics and [2]Division of Pathology, Cincinnati Children's Hospital Research Foundation, Cincinnati; and [3]Genzyme, Cambridge, MA

Lysosomal acid lipase (LAL) is the critical enzyme for the hydrolysis of triglycerides (TGs) and cholesteryl esters (CEs) in lysosomes. LAL defects cause Wolman disease (WD) and CE storage disease (CESD). An LAL null ($lal^{-/-}$) mouse model closely mimics human WD/CESD, with hepatocellular, Kupffer cell and other macrophage, and adrenal cortical storage of CEs and TGs. The effect on the cellular targeting of high-mannose and complex oligosaccharide–type oligosaccharide chains was tested with human LAL expressed in *Pichia pastoris* (phLAL) and CHO cells (chLAL), respectively. Only chLAL was internalized by cultured fibroblasts, whereas both chLAL and phLAL were taken up by macrophage mannose receptor (MMR)–positive J774E cells. After intraperitoneal injection into $lal^{-/-}$ mice, phLAL and chLAL distributed to macrophages and macrophage-derived cells of various organs. chLAL was also detected in hepatocytes. Ten injections of either enzyme over 30 d into 2- and 2.5-mo-old $lal^{-/-}$ mice produced normalization of hepatic color, decreased liver weight (50%–58%), and diminished hepatic cholesterol and TG storage. Lipid accumulations in macrophages were diminished with either enzyme. Only chLAL cleared lipids in hepatocytes. Mice double homozygous for the LAL and MMR deficiences ($lal^{-/-};MMR^{-/-}$) showed phLAL uptake into Kupffer cells and hepatocytes, reversal of macrophage histopathology and lipid storage in all tissues, and clearance of hepatocytes. These results implicate MMR-independent and mannose 6-phosphate receptor–independent pathways in phLAL uptake and delivery to lysosomes in vivo. In addition, these studies show specific cellular targeting and physiologic effects of differentially oligosaccharide-modified human LALs mediated by MMR and that lysosomal targeting of mannose-terminated glycoproteins occurs and storage can be eliminated effectively without MMR.

Introduction

Lysosomal acid lipase (LAL) hydrolyzes cholesteryl esters (CEs) and triglycerides (TGs) that are delivered to the lysosomes by receptor-mediated endocytosis (Goldstein et al. 1975). Mutations in the LAL gene cause two distinct phenotypes, Wolman disease (WD [MIM +278000]) and CE storage disease (CESD [MIM +278000]) (Assmann and Seedorf 2001). WD is a rare infantile-onset disorder, with an incidence of <1/300,000 live births (Meikle et al. 1999). Infants with WD display hepatosplenomegaly with massive accumulation of macrophages filled with CEs and TGs in the liver, spleen, and other organs. In addition, accumulation of CEs in the zona reticularis of the adrenal gland leads to adrenal calcification and insufficiency (Assmann and Seedorf 2001). Patients with WD develop cachexia from malabsorption related to the accumulation of engorged macrophages in the villi of the small intestine (Assmann and Seedorf 2001). The life span of patients with WD is ~6 mo. Bone marrow transplantation has had only minimal therapeutic impact (Krivit et al. 2000). CESD is a later-onset disorder and has been reported more frequently than WD. The incidence rate is unknown, but the disorder appears to be 2–3 times more common than WD. Hepatomegaly can be the only clinical manifestation. This results primarily from the accumulation of macrophages engorged with CEs (Beaudet et al. 1977). Some patients progress to develop cirrhosis, cholestasis, and atherosclerosis due to impaired cholesterol and TG homeostasis (Beaudet et al. 1977).

Deletions, insertions, or nonsense mutations in the LAL locus lead to WD with very low or absent LAL activity (Grabowski et al. 2003). In comparison, mutations found in patients with CESD have been missense changes or deletions localized to exon 10. These lead to small deletions in the C-terminus of the LAL protein (Grabowski et al. 2003). The milder CESD phenotypes correlate with the presence of detectible amounts of re-

Received July 7, 2005; accepted for publication October 3, 2005; electronically published October 27, 2005.

Address for correspondence and reprints: Dr. Gregory A. Grabowski, Cincinnati Children's Hospital Research Foundation, Division and Program in Human Genetics, 3333 Burnet Avenue, Cincinnati, OH 45229-3039. E-mail: greg.grabowski@cchmc.org

0002-9297/2005/7706-0016$15.00

sidual enzyme activity (Aslanidis et al. 1996; Redonnet-Vernhet et al. 1997). Although bone marrow transplantation has been used for WD therapy, therapeutic efforts for CESD have focused on diminishing the accumulation of CEs within the liver and spleen by use of hepatic 3-hydroxy-3-methylglutaryl coenzyme A (HMG-CoA) reductase inhibitors. Some effects on lipoprotein metabolism have been observed, but no demonstrable phenotypic or outcome effects have been reported consistently for these agents (Ginsberg et al. 1987).

An LAL null mouse model ($lal^{-/-}$) was created by gene targeting (Du et al. 1998*a*). The $lal^{-/-}$ mice have age-dependent progressive accumulation of CEs and TGs in the liver, spleen, small intestine, adrenal gland, and lymph nodes. The liver, small intestines, and lymph nodes are engorged with foamy macrophages filled with CEs and TGs. By age 6 mo, the $lal^{-/-}$ mice also show complete loss of white and brown adipose tissue throughout the body (Du et al. 2001*a*). These mice have a condition biochemically similar to WD but have survived into early adulthood (~8 mo life span).

Enzyme and gene strategies have been tested for therapeutic effects in the $lal^{-/-}$ mouse model (Du et al. 2001*b*, 2002). Human LAL (hLAL) produced in *Pichia pastoris* (phLAL) has shown promising results. Peritoneal administration of phLAL into $lal^{-/-}$ mice resulted in significant reductions of hepatomegaly and lipid storage in the liver, spleen, and small intestine. Interestingly, the reduction of lipid storage in the liver was primarily in Kupffer cells, whereas the lipid storage in the hepatic parenchymal cells was mostly unchanged (Du et al. 2001*b*). Such an effect might be expected from phLAL, because glycoproteins produced in this yeast have α-mannosyl–terminated N-linked oligosaccharides (Trimble et al. 2004). Adenoviral gene therapy in $lal^{-/-}$ mice was tested by single intravenous injections of recombinant virus containing the hLAL cDNA. The hLAL was produced primarily in the liver, with secretion into the bloodstream and uptake by visceral tissues (Du et al. 2001*b*). Significant corrections of lipid storage in the liver (Kupffer cells and hepatocytes), spleen, and small intestine were observed by histological and biochemical analyses (Du et al. 2002).

Here, the cellular targeting and physiologic effects of phLAL and of hLAL expressed in CHO cell lines (chLAL) are compared in $lal^{-/-}$ mice with and without intact macrophage mannose receptors (MMRs). Administration of phLAL or chLAL to $lal^{-/-}$ mice with intact MMR reduced lipid storage in macrophages. chLAL also reduced lipid storage in hepatocytes. In mice with both LAL and MMR disrupted, phLAL produced improvements in hepatocytes and visceral macrophages. These results provide insights into the effects of differential carbohydrate modifications on cellular targeting and biological activity, as well as the redistribution of glycoproteins by mechanisms other than mannose 6-phosphate (M6P) receptors and MMRs.

Material and Methods

Animals

The mice were provided care in accordance with institutional guidelines, and all protocols were approved by the Institutional Animal Care and Use Committee at the Children's Hospital Research Foundation. The $lal^{-/-}$ mice originated from mixed genetic backgrounds of 129Sv, CF-1, and FVB (Du et al. 1998*a*) and were backcrossed to a FVB background for 10 generations. The $MMR^{-/-}$ mice were a gift from Dr. Michel Nussenzweig, a Howard Hughes Medical Institute Investigator at The Rockefeller University (Lee et al. 2002). The $lal^{-/-};MMR^{-/-}$ double-knockout mice were generated by crossbreeding of $lal^{-/-}$ and $MMR^{-/-}$ mice in a C57BL/6 background. Mice were housed in microisolators, under 12 h/12 h dark/light cycles. Water and food (regular chow diets) were available ad libitum. The mice were genotyped by PCR-based screening of tail DNA (Du et al. 1998*a*; Lee et al. 2002).

Study Design

Three cohorts of age-matched $lal^{-/-}$ mice received 79 μg of phLAL, chLAL, or PBS injections. Two cohorts of age-matched $lal^{-/-};MMR^{-/-}$ mice received phLAL or PBS injections. Intraperitoneal (IP) injections were used in these studies, to mimic the slow infusion of enzyme replacement therapy in patients (Barton et al. 1991), rather than the intravenous boluses used in previous mouse studies. The injections of phLAL or chLAL were given to each mouse every 3 d for 30 d, for a total of 10 injections. Enzyme protein was quantified by immunoblotting assays (Du et al. 1998*b*). The $lal^{-/-}$ mice were harvested 2 d after the final injection, and tissues were processed for histologic, immunohistochemical, and biochemical analyses. phLAL activities were determined using 4-methylumbelliferyl-oleate (4-MUO) as substrate (Sheriff et al. 1995). All assays were conducted in duplicate. Assays were linear within the time frame used, and <10% of substrate was cleaved. One U is equal to 1 μM of 4-MUO cleaved per min under standard assay conditions (Sheriff et al. 1995).

Enzyme Uptake Studies in J774E Macrophages and Human Fibroblast Cultures

J744E cells expressing MMR (from Dr. Philip Stahl at Washington University, St. Louis) were used previously for cellular uptake of phLAL (Du et al. 2001*b*). J774E cells were maintained in minimal essential medium with 6-thioguanine (60 μM), and human fibro-

blasts were maintained in Dulbecco's minimal essential medium supplemented with 10% fetal calf serum, penicillin, and streptomycin (at 37°C; 5% CO_2). For the uptake studies, cells (2×10^5 per well) were seeded 1 d before the addition of phLAL or chLAL. The cells were incubated in medium containing phLAL or chLAL, with or without M6P, for 24 h and then in fresh media without LAL and were harvested at 48 h. The cells were washed twice with 1× PBS, were collected with a cell scraper, and were centrifuged (at 12,000 rpm for 1 min) at room temperature. The intracellular proteins were extracted by cell lysis (10 mM $NaPO_4$, 1 mM EDTA, 10 mM dithiothreitol, and 0.5% NP-40; pH 6.8) with sonication and were centrifuged (at 12,000 rpm for 10 min) at 4°C. The protein extracts were analyzed by western blot.

Immunohistochemical Staining and Western Blot Analyses

Immunohistochemical analyses of paraffin-embedded tissue sections were performed as described elsewhere (Du et al. 2001*b*). From the VECTASTAIN ABC kit (Vector), a second antibody to rabbit anti-hLAL antiserum (Du et al. 1996) was used and counterstained with Nuclear Fast Red. Immunoblots were conducted with anti-hLAL antiserum, as described elsewhere (Du et al. 2001*b*). The intracellular form of hLAL on western blots was evaluated by densitometry scanning (Pharmacia LKB Ultroscan XL).

Tissue Lipid Analyses

Total lipids were extracted from liver, spleen, and small intestine by the Folch method (Folch et al. 1957; Du et al. 1998*a*). TG and cholesterol amounts were measured by chemical analysis (Rudel and Morris 1973; Du et al. 2001*a*).

Histologic Analyses

Light-microscopic examinations of the liver, spleen, intestine, and adrenal glands were performed. The paraffin-embedded sections were stained with hematoxylin and eosin (H+E) for light-microscopic analysis. Representative sections are presented.

Monosaccharide Composition Analyses

The monosaccharide composition of the oligosaccharide structures in LAL samples was determined by acid hydrolysis. Purified phLAL (80 μg) was incubated with 250 μl of 2-M trifluoroacetic acid at 120°C for 2 h. After hydrolysis, the reaction tubes were cooled on ice, were centrifuged (at 10,000 rpm for 1 min), and were evaporated to dryness in a vacuum centrifuge. The released monosaccharides were separated by high-pH anion exchange chromatography coupled with pulsed amperometric detection (HPAEC-PAD) on a Dionex CarboPac PA1 (4 × 250 mm) column equilibrated and run in 24 mM sodium hydroxide at a flow rate of 1 ml/min for 20 min. The results were expressed as mole of sugar per mole of LAL and were determined from linear curves of authentic, commercially available monosaccharide standards (E Y Laboratories).

M6P Content

The M6P content of the oligosaccharide structures in LAL samples were determined by acid hydrolysis. phLAL (80 μg) was incubated with 6.75 M formic acid at 100°C for 1.5 h. After incubation, samples were cooled, dried in a vacuum centrifuge, and reconstituted in distilled water (200 μl). The released M6P was analyzed by HPAEC-PAD on a Dionex CarboPac PA10 (4 × 250 mm; Dionex) column by use of a 170–400-mM sodium acetate gradient in 100 mM sodium hydroxide at a flow rate of 1 ml/min for 15 min. The results were expressed as mol of M6P per mol of LAL and were determined from linear curves of authentic, commercially available M6P standards.

Sialic Acid Content

The sialic acid content of the oligosaccharide structures in LAL samples was determined by mild acid hydrolysis. LAL (50 μg) was incubated in 0.5 M formic acid (at 80°C for 60 min). The released sialic acids were separated by HPAEC-PAD on a Dionex CarboPac PA1 (4 × 250 mm) column by use of a 50–180-mM sodium acetate gradient in 100 mM sodium hydroxide at a flow rate of 1 ml/min for 20 min. The results were expressed as mol of sialic acid per mol of LAL and were determined from linear curves of authentic, commercially available sialic acid standards (Toronto Research).

Oligosaccharide Profiling

The N-linked oligosaccharides were released from chLAL and phLAL samples by use of 0.2% (6 U/mg) of PNGase F and 2-mercaptoethanol (57.2 mM) in sodium phosphate, pH 7.0, at 37°C for 18–20 h. To separate the deglycosylated protein from the released oligosaccharides, the digests were centrifuged (at 14,000 rpm for 30 min) using a 10-kDa molecular weight–cutoff regenerated cellulose membrane spin-filters. The filtrates containing the oligosaccharides were dried in a vacuum centrifuge for at least 4 h. The oligosaccharides were reconstituted in 500 μl of high-performance liquid chromatography (HPLC)–grade water and were dialyzed using a 1-kDa molecular weight–cutoff cellulose acetate membrane against sodium phosphate, pH 7.0, at 25°C for 18–20 h. The dialysate was dried in a vacuum centrifuge, was reconstituted in 50 μl HPLC-grade water,

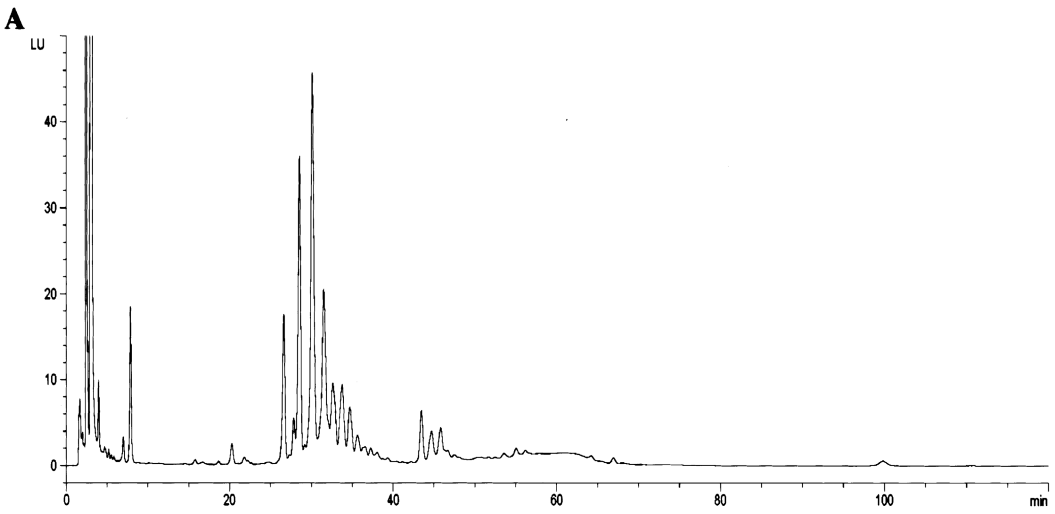

Proposed structures of phLAL-derived oligosaccharides:

Retention Time	Propsed Structure (based on mass)
26.9	$Man_8GlcNAc_2$
28.0	$Man_9GlcNAc_2$
28.9	$Man_9GlcNAc_2$
30.4	$Man_{10}GlcNAc_2$
31.7	$Man_{11}GlcNAc_2$
33.1	$Man_{12}GlcNAc_2$
34.2	$Man_{13}GlcNAc_2$
34.9	$Man_{14}GlcNAc_2$
36.1	$Man_{15}GlcNAc_2$
43.7	$Man_{12}GlcNAc_2$
45.3	$Man_{11}GlcNAc_2+ PO_4$, $Man_{10}GlcNAc_2+ PO_4$
46.2	$Man_{11}GlcNAc_2+ PO_4$, $Man_{12}GlcNAc_2+ PO_4$, $Man_{13}GlcNAc_2+ PO_4$
100.6	$Man_7GlcNAc_2+ 2PO_4$

Figure 1 HPLC profiles of AA-derivatized phLAL-derived (*A*) and chLAL-derived (*B*) oligosaccharides. The proposed structures of oligosaccharides are listed below each respective graph. LU = Luminescence units.

and was labeled with anthranilic acid (Van Dongen et al. 1984).

The oligosaccharides were derivatized using the protocol described by Anumula and Dhume (1998). In brief, the released oligosaccharides were resuspended in 0.1 ml HPLC-grade water and were labeled with 0.1 ml of labeling solution (30 mg anthranilic acid and 25 mg sodium cyanoborohydride in 1 ml of 4% sodium acetate and 2% boric acid in methanol) at 80°C for 75 min. After the labeling, the reactions were quenched with 1 ml of 95% acetonitrile/5% water and were loaded onto the Oasis HLB cartridges (Waters Corporation). The excess reagents were removed using 2 × 1-ml washes of 95% acetonitrile/5% water. Derivatized oligosaccharides were eluted using 0.5 ml of 20% acetonitrile/80% water, were dried, and were resuspended in 125 μl of 20% acetonitrile prior to HPLC analyses.

The AA-labeled oligosaccharides (100 μl sample/injection) were separated on a Luna NH2 column (4.6 × 250 mm; Phenomenex) by use of an HP1100 system equipped with a fluorescent detector (peak excitation wavelength at 230 nm; peak emission wavelength at 425 nm). The column was equilibrated in 70% solvent A (2% acetic acid and 1% inhibited tetrahydrofuran in acetonitrile), and the AA-labeled oligosaccharides were eluted at 50°C by use of a gradient consisting of 30%–95% of solvent B (5% acetic acid, 3% triethylamine, and 1% inhibited tetrahydrofuran in water) at a flow rate of 1 ml/min for 80 min. The gradient was held at 95% solvent B for an additional 38 min, to elute the bisphosphorylated species.

The HPLC chromatographic eluant containing the AA-derivatized peaks were split after column separation (~1:50) and were directly analyzed by electrospray ionization (ESI) mass spectrometry on a ZQ4000 mass spectrometer (Waters Corporation). The parameters on the mass spectrometer were capillary voltage at 3.0 kV and cone voltage at −30 V. The negative-ion ESI mass spec-

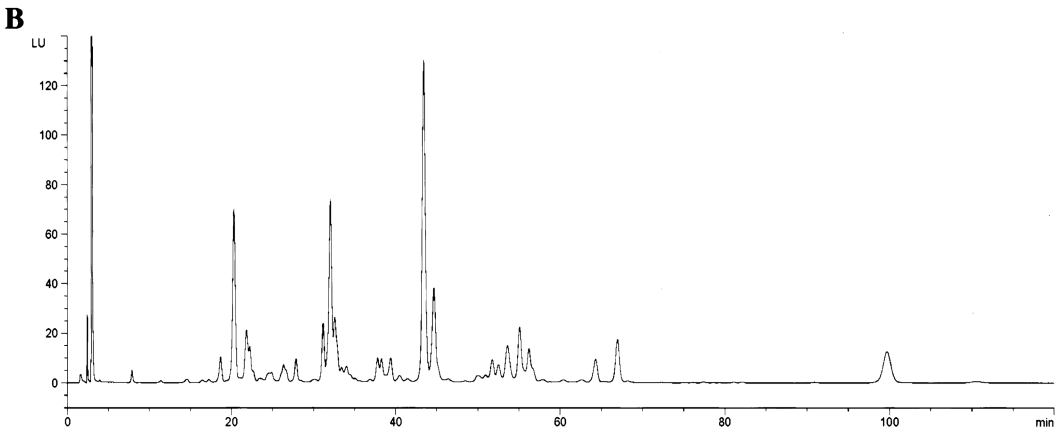

Proposed structures of chLAL-derived oligosaccharides:

Retention Time	Proposed Structure (based on mass)
18.9	$Man_3GlcNAc_2$ + Fucose
20.5	$Man_5GlcNAc_2$, $Man_3GlcNAc_4Gal$ + Fucose
22.2	$Man_3GlcNAc_4Gal_2$ + Fucose
22.7	$Man_7GlcNAc_2$
25.5	$Man_7GlcNAc_2$
26.5	$Man_8GlcNAc_2$
28.3	$Man_9GlcNAc_2$
31.5	$Man_3GlcNAc_4Gal$ + Fucose + Sialic acid (NeuAc)
32.3	$Man_3GlcNAc_4Gal_2$ + Fucose + Sialic acid (NeuAc) , $Man_3GlcNAc_4Gal$ + Sialic acid (NeuAc)
34.1	$Man_5GlcNAc_2Gal$ + Fucose + Sialic acid (NeuAc), $Man_3GlcNAc_5Gal_3$ + Fucose + Sialic acid (NeuAc)
43.7	$Man_3GlcNAc_4Gal_2$ + Fucose + Sialic acid ($NeuAc_2$)
44.9	$Man_3GlcNAc_4Gal_2$ + $NeuAc_2$
52.1	$Man_7GlcNAc_3$ + PO_4
52.6	$Man_6GlcNAc_3$ + PO_4
53.9	$Man_6GlcNAc_2$ + PO_4
55.4	$Man_3GlcNAc_5Gal_3$ + Fucose + Sialic acid ($NeuAc_3$) , $Man_6GlcNAc_2$ + PO_4
56.4	$Man_3GlcNAc_5Gal_3$ + Fucose + Sialic acid ($NeuAc_3$)
67.3	$Man_6GlcNAc_3Gal$ + Fucose + Sialic acid (NeuAc) + PO_4
99.4	$Man_7GlcNAc_2$+ $2PO_4$

tra were obtained over a mass range of 500–3,750 m/z at an interval of 5 s per scan. The resulting mass spectra were obtained by summing at least six scans.

Results

Expression of phLAL and chLAL

phLAL was produced in *P. pastoris* by use of the yeast GAPDH promoter and the α factor signal peptide. chLAL was produced in a CHO cell line by use of the mouse metallothionine promoter and the hLAL endogenous leader sequence. phLAL and chLAL were secreted into culture media and were purified to 93%–96% electrophoretic purity as assessed by SDS-PAGE.

Oligosaccharide Profiling

The N-linked oligosaccharides from phLAL and chLAL samples were released using PNGase F, were fluorescently labeled with anthranilic acid, and were analyzed by liquid chromatography with online mass spectrometry. On the basis of mass:charge ratios, phLAL contained predominantly high-mannose structures: from $Man_8GlcNAc_2$ to $Man_{15}GlcNAc_2$. The most abundant oligosaccharide structures in phLAL were $Man_{8-12}GlcNAc_2$ (fig. 1*A*, retention time ~28–33 min). In CHO cells, secreted high-mannose N-glycans ($Man_9GlcNAc_2$ and smaller) are observed at low levels, since most of these structures typically get processed into $Man_5GlcNAc_2$ glycans during passage through the endoplasmic reticulum and Golgi compartments. In contrast to CHO cells, *P. pastoris* cells add mannose to this structure to produce high-mannose N-glycans, with up

to 15 mannose residues. However, in both phLAL and chLAL, some of the structures get modified by a GlcNAc-phosphotransferase, and the GlcNAc residues are subsequently removed, yielding phosphorylated structures. Some of the high-mannose structures in phLAL were either monophosphorylated ($Man_{10–13}GlcNAc_2$, retention times ~43–46 min) or bisphosphorylated ($Man_7GlcNAc_2$, retention times ~100 min).

The glycans from chLAL consisted of a mixture of complex (sialylated), oligomannose, phosphorylated oligomannose, and hybrid (sialylated and phosphorylated) structures (fig. 1*B*). The presence of galactose, sialic acid, and M6P in the carbohydrate composition assay confirms these glycan structures. The phosphorylated structures in chLAL were mainly $Man_{6–7}GlcNAc_2$, some of which still had the additional GlcNAc residue from the transferase activity. In phLAL and chLAL, compositionally identical glycans eluted at different retention times during the chromatographic separation—for example, in phLAL, $Man_9GlcNAc_2$ eluted at ~28–29 min, and, in chLAL, $Man_7GlcNAc_2$ eluted at ~23–26 min. This may be because of the different isomeric forms of the glycan, which would have the same mass:charge ratios in this assay.

Monosaccharide Composition and Sialic Acid and M6P Content of phLAL and chLAL Oligosaccharides

The oligosaccharide compositions of phLAL and chLAL were analyzed after acid hydrolysis and separation by HPAEC-PAD (table 1). Monosaccharide compositional analyses indicated that chLAL and phLAL contained ~10 mol of GlcNAc per mol of LAL, suggesting that five of six potential N-linked oligosaccharide sites are occupied. The number of experimentally determined mannose residues (~10) does not correlate with the number predicted for five occupied sites (15 mannoses would be expected if all were complex oligosaccharides). The less-than-expected mannose results may be because of the fact that the monosaccharide compositional analysis is highly variable. Also, the monosaccharide/protein (M/M) results differ from the theoretical values calculated from the actual identified oligosaccharide structures. The chLAL sample had higher amounts of fucose and galactose, corroborating the presence of complex-type structures. The phLAL sample had higher amounts of mannose that correlated with either high-mannose or pauci-mannosyl structures

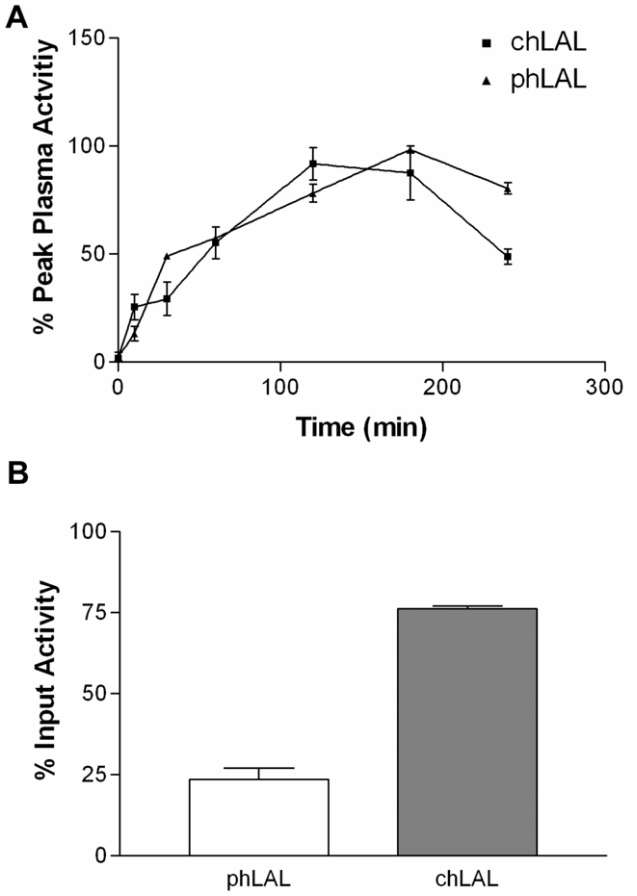

Figure 2 LAL activity in plasma (*A*) and LAL activity recovery in liver (*B*) of *lal*$^{-/-}$ mice that received IP injections of hLAL. Plasma was collected from phLAL- or chLAL-injected mice at 0, 10, 30, 60, 120, 180, and 240 min after injection. Livers were collected at 240 min after injection. LAL activities in plasma and liver extract were determined using 4-MUO as the substrate.

in *P. pastoris*–derived samples. The phLAL samples contained no galactose. Although the monosaccharide results indicated that phLAL contained minimal sialic acid, it is well understood that *P. pastoris,* like plants, does not possess the necessary enzymes (β1,4 galactosyltransferases and α2,3 sialyltransferases) to remodel N-linked glycosylation of oligosaccharide chains (Lerouge et al. 1998; Montesino et al. 1998). The lack of sialylated glycan structures was confirmed in the oligosaccharide profiling assay (see the "Oligosaccharide Profiling" section). Both phLAL and chLAL contained phosphoryl-

Table 1

Monosaccharide Composition and M6P and Sialic Acid Content (per mol of hLAL Protein)

Sample	Fucose	GlcNac	Galactose	Mannose	GlcNac/Mannose	M6P	Sialic Acid
phLAL	.6	10.0	0	212.0	.05	1.7	.5
chLAL	1.5	11.6	4.1	10.4	1.11	2.2	5.9

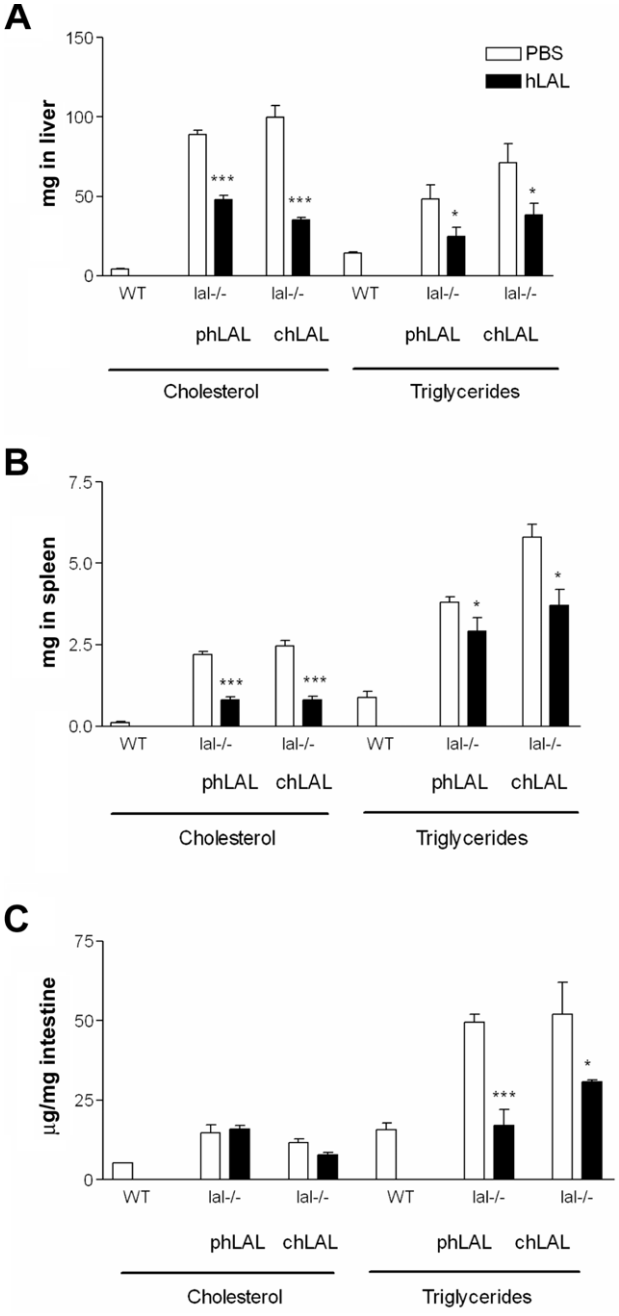

Figure 3 Tissue cholesterol and TGs in $lal^{-/-}$ mice administered PBS or chLAL. Total cholesterol or total TGs per liver (*A*) or per spleen (*B*) and lipid concentration in intestine (*C*) was compared between PBS control mice and phLAL- or chLAL-injected mice ($n = 6$). The *P* values were from unpaired *t* tests between PBS and chLAL-treated samples. $^{*}P < .05$. $^{***}P < .001$. WT = wild type.

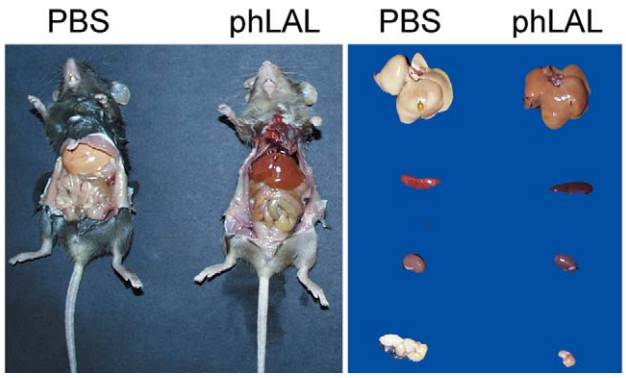

Figure 4 Gross pathology of age-matched PBS and phLAL-treated $lal^{-/-};MMR^{-/-}$ mice. Ventral views (*left panel*) show the yellow fatty liver in PBS control $lal^{-/-};MMR^{-/-}$ mice. In phLAL-treated $lal^{-/-};MMR^{-/-}$ mice, the liver had essentially normal color. Gross view of livers, spleens, kidneys, and mesenteric lymph nodes (*right panel, top to bottom*) from PBS and phLAL-treated $lal^{-/-};MMR^{-/-}$ mice. Notice that the color of these organs was nearly normal in phLAL-treated $lal^{-/-};MMR^{-/-}$ mice.

ated oligomannosyl structures (1.7 and 2.2 mol M6P per mol protein, respectively). This amount of M6P is similar to values reported in the literature for other recombinant CHO-derived proteins that are taken up by the lysosomes via the M6P receptor system (Lee et al. 2003).

Plasma Profiles of Injected hLAL

The recovery of hLAL activity in plasma was determined after IP injection into $lal^{-/-}$ mice with intact MMR and the sampling of blood at 0, 10, 30, 60, 120, 180, and 240 min after injection. The profiles (fig. 2*A*) of phLAL and chLAL in plasma were essentially identical for activities remaining in plasma from 15 to 240 min. The total LAL activity recovered in the liver at 4 h after injection was significantly greater for chLAL (76.3%) than for phLAL (23.5%) (fig. 2*B*).

Phenotypic and Gross Pathologic Changes

To evaluate the metabolic effects of each hLAL, $lal^{-/-}$ mice were injected with PBS, phLAL, or chLAL (79 µg per dose) every third day over a 30-d period, for a total of 10 IP injections. phLAL was started at age 2 mo, and chLAL was started at age 2.5 mo. The PBS control group was staggered between the 2- and 2.5-mo-old mice. This small age difference does not produce a significantly different degree of disease involvement. Untreated $lal^{-/-}$ mice developed a yellow coloration of the liver, as well as significant hepatosplenomegaly. The $lal^{-/-}$ mice receiving phLAL or chLAL had livers with more normal color and weight (data not shown). The livers in age-matched wild-type mice were ~5% of body

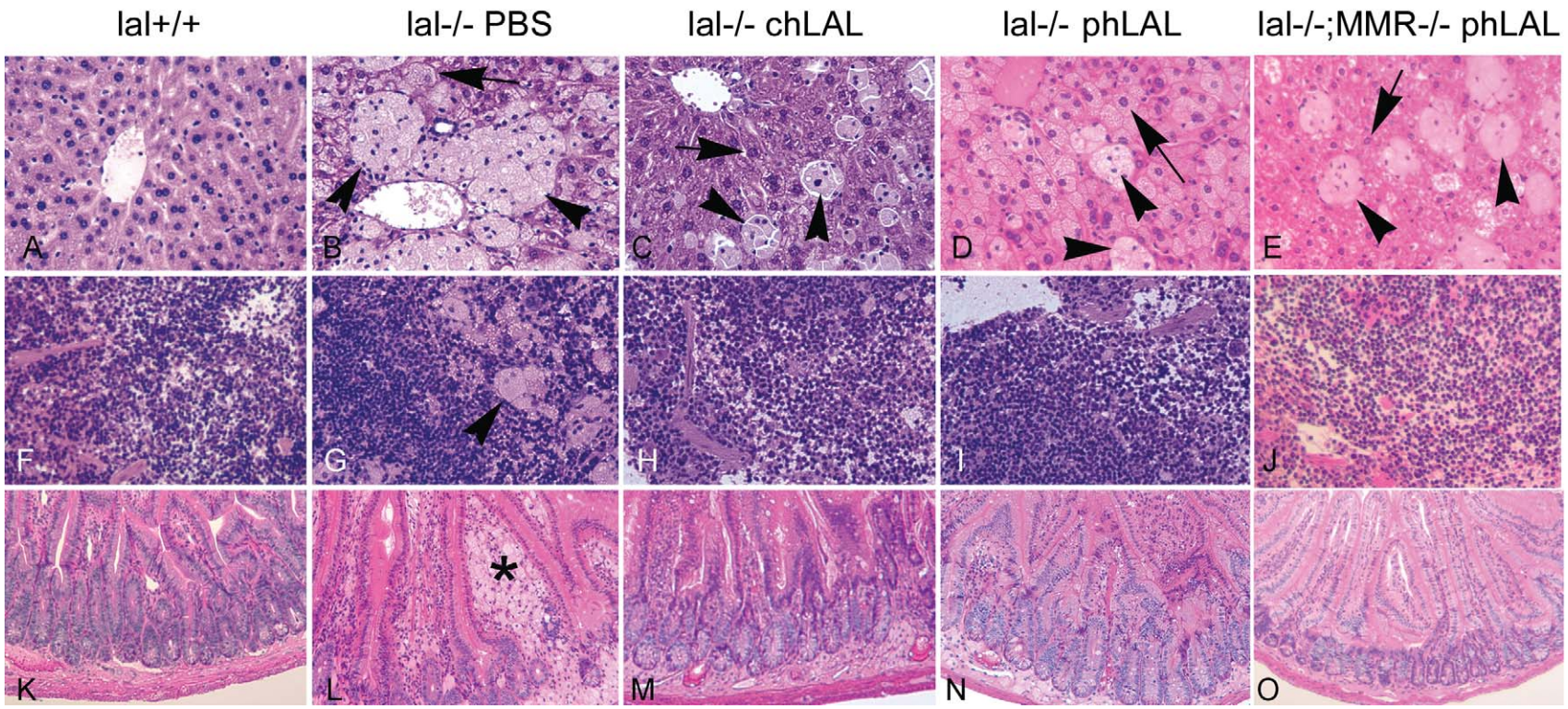

Figure 5 Histological analyses of wild-type, $lal^{-/-};MMR^{+/+}$, and $lal^{-/-};MMR^{-/-}$ mice administered PBS, phLAL, or chLAL. Shown are representative H+E-stained tissue sections from age-matched wild-type ($lal^{+/+}$) mice (*A, F,* and *K*); from $lal^{-/-};MMR^{+/+}$ mice injected with PBS (*B, G,* and *L*), chLAL (*C, H,* and *M*), or phLAL (*D, I,* and *N*); and from $lal^{-/-};MMR^{-/-}$ mice treated with phLAL (*E, J,* and *O*). The tissues are liver (*A–E*), spleen (*F–J*), and small intestine (*K–O*). Arrows indicate hepatocytes, arrowheads indicate Kupffer cells, and the asterisk (*) indicates intestinal macrophages. The numbers of remaining Kupffer storage cells in the phLAL- or chLAL-treated mouse livers are similar, whereas the hepatocytes in the chLAL-treated $lal^{-/-};MMR^{+/+}$ mice and the phLAL-treated $lal^{-/-};MMR^{-/-}$ mice are essentially cleared of storage. Hepatocyte storage remained in the phLAL-treated $lal^{-/-};MMR^{+/+}$ mice. In spleen and small intestine, the storage macrophages were nearly eliminated in all phLAL-treated mice. Original magnification, ×200.

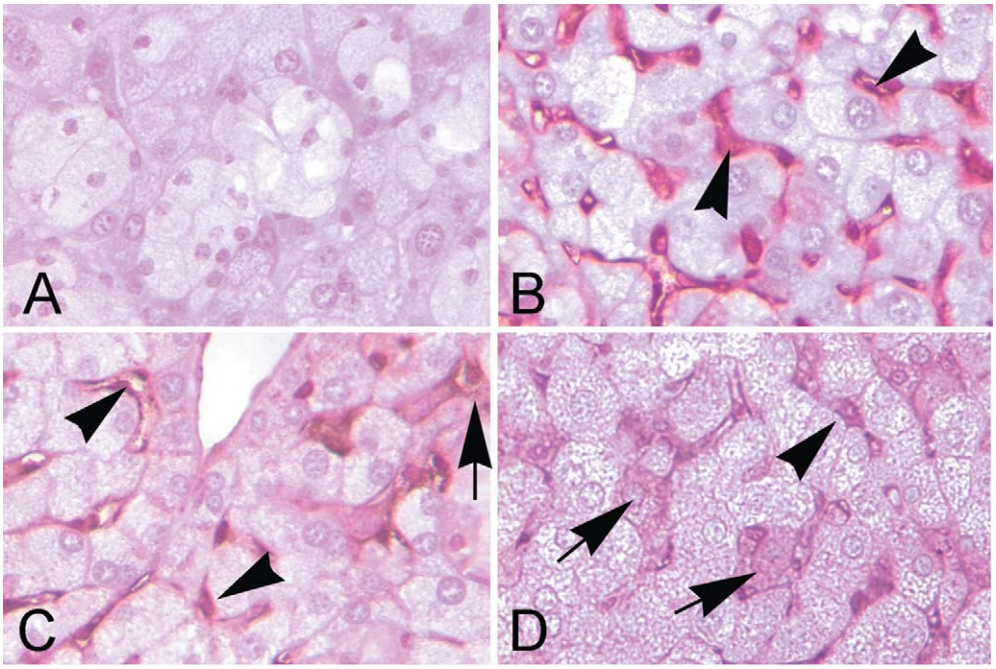

Figure 6 Anti-hLAL immunohistochemical staining of $lal^{-/-};MMR^{+/+}$ (*A–C*) and $lal^{-/-};MMR^{-/-}$ (*D*) mouse livers. $lal^{-/-};MMR^{+/+}$ mice were given IP injections of PBS (*A*), phLAL (*B*), and chLAL (*C*), and $lal^{-/-};MMR^{-/-}$ mice were given IP injections of phLAL (*D*). The amount of hLAL given to each mouse was 79 μg. Mice were killed 4 h after injection. Liver and spleen were processed for immunohistochemical staining by use of anti-hLAL antibody. Positive signals were in Kupffer cells of the livers (*B–D*, *arrowheads*) and in hepatocytes (*C* and *D*, *arrows*). Original magnification, ×400.

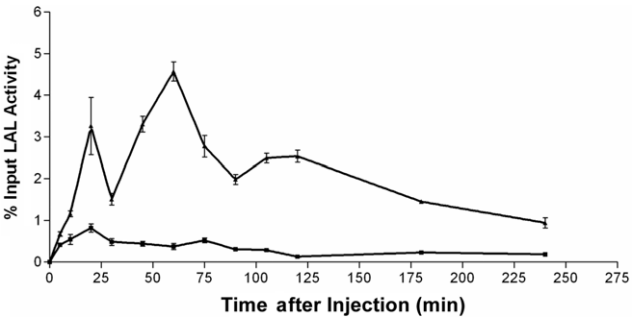

Figure 7 Comparison of plasma LAL activity between wild-type and $MMR^{-/-}$ mice after a single injected dose of hLAL. Age-matched wild-type (*lower line*) and $MMR^{-/-}$ (*upper line*) mice received a single dose (60 μg phLAL per 25 g body weight) via IP injection. Plasma was collected from mice at 0, 5, 20, 30, 45, 60, 75, 90, 105, 120, 180, and 240 min after injection. LAL activities in plasma were determined using 4-MUO as the substrate. Plasma volume was calculated as 3.5% of body weight. The percentage activity remaining in plasma, with respect to input LAL activity, was plotted against time.

weight, whereas the livers in the untreated $lal^{-/-}$ mice were ~14%. In phLAL- and chLAL-injected mice, the livers were 9.8% (reduced by 30%; $P = .0029$) and 7.7% (reduced by 45%; $P = .0001$) of body weight, respectively.

Biochemical Findings

Tissue cholesterol (free and esterified) and TGs from liver, spleen, and small intestine were evaluated in treated and untreated $lal^{-/-}$ mice (fig. 3). Administration of phLAL to $lal^{-/-}$ mice led to 46% reduction in total hepatic cholesterol (48.08 ± 2.67 mg [treated] vs. 89.07 ± 2.74 mg [untreated]; $P = .0003$; $n = 4$) (fig. 3*A*) and 63% reduction in total splenic cholesterol (0.80 ± 0.10 mg vs. 2.19 ± 0.10 mg; $P = .0008$; $n = 4$) (fig. 3*B*). Similar decreases in TGs were observed: 49% reduction in liver (24.84 ± 5.79 mg vs. 48.26 ± 8.97 mg; $P = .025$; $n = 4$) and 24% reduction in spleen (2.90 ± 1.43 mg vs. 3.80 ± 0.17 mg; $P = .042$; $n = 4$) (fig. 3*A* and 3*B*). Administration of chLAL to $lal^{-/-}$

mice resulted in reductions of total hepatic and splenic cholesterol by 65% (35.19 ± 1.55 mg vs. 99.94 ± 7.13 mg; $P < .0001$; $n = 6$) (fig. 3*A*) and 67% (0.80 ± 0.13 mg vs. 2.45 ± 0.17 mg; $P = .0012$; $n = 6$) (fig. 3*B*), respectively. The reduction of TGs was 47% in the liver and 36% in the spleen ($P = .040$ and $P = .017$, respectively) (fig. 3*A* and 3*B*). The cholesterol accumulation in small intestine was unchanged by phLAL or chLAL administration. However, the TG storage in small intestine was reduced by 66% and 41% with administration of phLAL and chLAL, respectively (fig. 3*C*). Lipids in the massively enlarged mesenteric lymph nodes were not significantly changed (3.72 ± 0.17 mg vs. 4.28 ± 0.7 mg for total cholesterol; 21.74 ± 5.59 vs. 16.53 ± 2.99 mg for TGs).

Effects of phLAL Injections into lal$^{-/-}$;MMR$^{-/-}$ *Mice*

To evaluate the role of MMR as a major receptor mediating the therapeutic effects of highly mannosylated phLAL, double-homozygous knockouts were generated for *lal*$^{-/-}$ and *MMR*$^{-/-}$. The phenotype of *lal*$^{-/-}$ mice was not altered in the background of *MMR*$^{-/-}$. Administration of phLAL (79 μg per mouse, 10 IP injections given over 30 d) effectively corrected the phenotype in *lal*$^{-/-}$;*MMR*$^{-/-}$ mice. This included the correction of liver and spleen color and the reappearance of mesenteric fat (fig. 4). The liver as a percentage of body weight was reduced in phLAL-treated *lal*$^{-/-}$;*MMR*$^{-/-}$ mice (11.1% in mice given PBS vs. 8.8% in mice given phLAL; −21%). Even more striking was the reduction in the size of mesenteric lymph nodes in the phLAL-treated mice compared with PBS control mice (0.273 g in control mice vs. 0.081 g in phLAL-treated mice; −70%)

Histologic Studies

Representative H+E-stained liver sections from *lal*$^{+/+}$ mice or *lal*$^{-/-}$ mice with or without MMR and obtained after PBS, chLAL, or phLAL administration are shown in figure 5. Regular phLAL injections led to major reductions in the size and number of lipid-filled Kupffer cells (arrowheads in fig. 5*B* and 5*D*) in *lal*$^{-/-}$;*MMR*$^{+/+}$ mice. In comparison, the lipid storage in hepatocytes appeared unaltered (arrows in fig. 5*B* and 5*D*). In the *lal*$^{-/-}$ mice treated with chLAL, a reduction was observed in the number and size of Kupffer storage cells, and lipid accumulation was eliminated from hepatocytes (arrow in fig. 5*C*). Interestingly, in *lal*$^{-/-}$;*MMR*$^{-/-}$ mice, injections of phLAL reduced the lipid storage in hepatocytes (arrows) and Kupffer cells (arrowheads) (compare fig. 5*B* and 5*E*). H+E staining of other tissues—that is, spleen and small intestine—indicated that phLAL and chLAL administration had similar effects in reducing

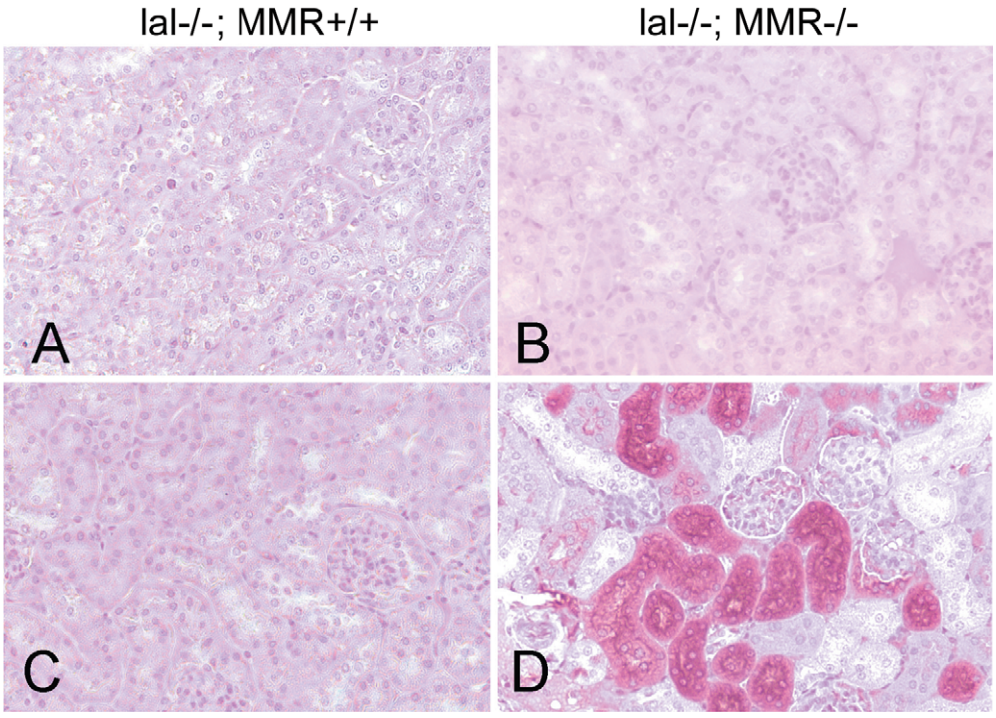

Figure 8 Anti-hLAL immunohistochemical staining of *lal*$^{-/-}$;*MMR*$^{+/+}$ (*A* and *C*) and *lal*$^{-/-}$;*MMR*$^{-/-}$ (*B* and *D*) mouse kidneys. Kidney sections from PBS-injected mice (*A* and *B*) and hLAL-injected mice (*C* and *D*) were processed for immunohistochemical staining by use of anti-hLAL antibody. Only *lal*$^{-/-}$;*MMR*$^{-/-}$ mice had positive uptake of hLAL in kidneys and only in the proximal renal tubular epithelial cells (*D*). Original magnification, × 200.

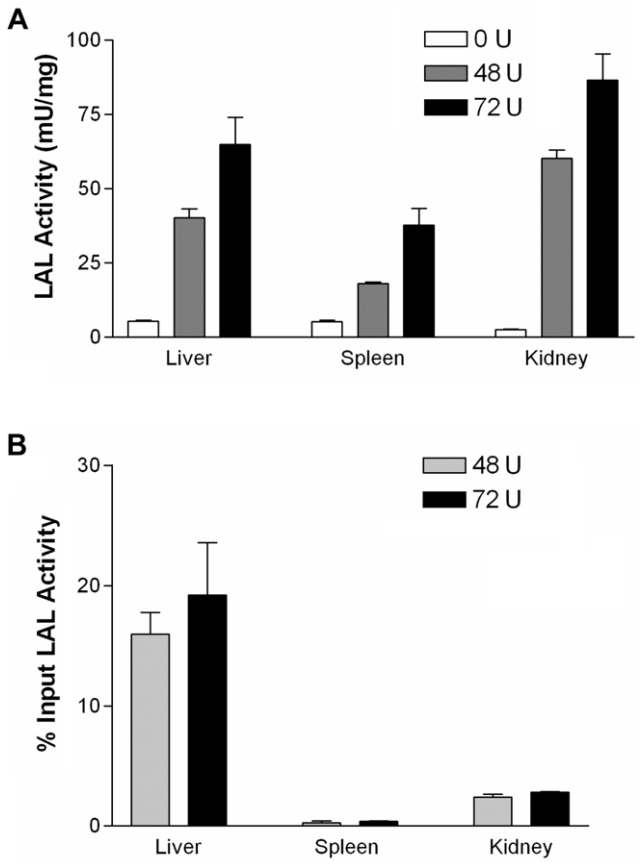

Figure 9 Tissues recovery of phLAL. *A*, LAL activity in tissue extracts of liver, spleen, and kidney from $lal^{-/-};MMR^{-/-}$ mice that received 48 U or 72 U of phLAL and were harvested 4 h after injection. *B*, LAL activity recovery in liver, spleen, and kidney as a percentage of total injected LAL activity in $lal^{-/-};MMR^{-/-}$ mice.

lipid-storage cells in $lal^{-/-};MMR^{+/+}$ and $lal^{-/-};MMR^{-/-}$ mice (fig. 5*F*–5*J* and 5*K*–5*O*). Similar to the results for phLAL, chLAL had no effect on lipid storage in lymph nodes and adrenal glands in $lal^{-/-};MMR^{+/+}$ mice (data not shown). Treatment with phLAL in $lal^{-/-};MMR^{-/-}$ mice had no histological effects on lipid storage in adrenal glands or lymph nodes, although there was a reduction in lymph node size (fig. 4).

Comparison of Cellular Uptake of phLAL and chLAL

To evaluate the cellular targeting of phLAL and chLAL in the $lal^{-/-};MMR^{+/+}$ and $lal^{-/-};MMR^{-/-}$ mice, livers were harvested and sectioned at 4 h after injection (79 μg per mouse) and were processed for immunohistochemical staining with the use of anti-hLAL antibody. The majority of positive-staining liver cells after injection of either phLAL or chLAL was in sinusoid-lining cells (arrowheads, fig. 6*B* and 6*C*). Some hepatocyte staining was also positive in chLAL-injected mice (arrow, fig. 6*C*). Interestingly, positive staining for phLAL in the liver of $lal^{-/-};MMR^{-/-}$ mice was less intense than that in livers of phLAL-injected $lal^{-/-};MMR^{+/+}$ mice. However, unlike injected $lal^{-/-};MMR^{+/+}$ mice, the $lal^{-/-};MMR^{-/-}$ mice had positive hLAL signals in both Kupffer cells and hepatocytes (arrowhead and arrows, respectively, in fig. 6*D*).

Plasma Pharmacokinetics of hLAL in $MMR^{+/+}$ and $MMR^{-/-}$ Mice

Since the deficiency of MMR in mice affects the uptake of multiple glycoproteins from plasma into tissues and organs (Lee et al. 2002), the pharmacokinetics of phLAL uptake was evaluated in $MMR^{+/+}$ and $MMR^{-/-}$ mice. After a single dose of phLAL, $MMR^{+/+}$ mice showed rapid uptake into tissues, with ~1% of injected LAL activity remaining in plasma after ~2 h. The $MMR^{-/-}$ mice displayed a complex plasma pharmacokinetic pattern, with two major peaks of activity at 15 and 60 min after injection (fig. 7). The clearance of LAL activity in plasma was very slow in $MMR^{-/-}$ mice, with significant enzyme activities remaining at 4 h after injection. To evaluate organ uptake of phLAL, immunohistochemical staining for hLAL was performed in $lal^{-/-};MMR^{+/+}$ and $lal^{-/-};MMR^{-/-}$ mice 4 h after injection. Interestingly, in addition to liver and spleen, the proximal renal tubular epithelial cells were strongly positive for LAL staining in the $lal^{-/-};MMR^{-/-}$ mouse kidney (fig. 8*D*). The kidneys were negative for hLAL staining after injection of phLAL into $lal^{-/-};MMR^{+/+}$ or of PBS into $lal^{-/-};MMR^{-/-}$ mice (fig. 8*B* and 8*C*). LAL activity in tissue extracts from $lal^{-/-};MMR^{-/-}$ mice indicated higher LAL-specific activity in the kidney than in the liver (fig. 9*A*), although the total recovery of phLAL was much less in the kidney than in the liver because of the size of the organs (fig. 9*B*). To further test whether the uptake of phLAL could be through the M6P receptor, phLAL and chLAL were incubated with human fibroblasts from an LAL-deficient patient or MMR-positive J774E cells. Human fibroblasts were negative for MMR and positive for M6P receptors. Uptake of chLAL occurred in MMR-positive J774E cells and M6P receptor–positive human fibroblasts (fig. 10*A*). The uptake of chLAL in fibroblasts can be competed with by M6P (fig. 10*B*). phLAL was internalized into J774E cells (Du et al. 2001*b*), but no uptake was observed in human fibroblasts (fig. 10*A*). The results show that the in vivo uptake of phLAL into a variety of cells can occur through receptors other than M6P receptors and MMRs.

Discussion

These data show differential glycosylation of IP-administered LALs that leads to specific physiologic and localization changes at a cellular level. These findings demonstrate that alternative oligosaccharide processing of

administered enzymes can lead to clear differential therapeutic effects at a cellular level. The presence of high mannose oligosaccharides on phLAL leads to preferential, if not exclusive, uptake by hepatic sinusoidal-lining cells, including Kupffer cells, and other visceral macrophages. This produced specific reductions of CE and TG storage in these cells of $lal^{-/-};MMR^{+/+}$ mice. In comparison, the enzyme produced in CHO cells, chLAL, led to clearance of CEs and TGs in hepatocytes, Kupffer cells, other hepatic sinusoidal lining cells, and macrophages throughout the bodies of such mice. Importantly, equal doses of phLAL produced similar degrees of reduction in storage cells and lipids in the mice lacking both *lal* and MMR (i.e., $lal^{-/-};MMR^{-/-}$ mice). However, the effects of phLAL in the background of $MMR^{-/-}$ produced significantly different clearance effects in the liver but not in other tissues. In the $lal^{-/-};MMR^{-/-}$ mice that received phLAL, the liver showed hepatocellular clearance in addition to significant reductions in lipid storage in Kupffer cells that were comparable to those in chLAL-treated $lal^{-/-};MMR^{+/+}$ mice. The clearance of storage macrophages from the spleen and small intestine by phLAL was essentially complete in $lal^{-/-};MMR^{-/-}$ and $lal^{-/-};MMR^{+/+}$ mice. Thus, the lack of MMR altered the physiological effect of the exogenous enzyme-containing high-mannose residues to include a major effect on hepatocytes as well as macrophages. This is somewhat surprising in light of the delayed clearance of mannose-terminated glycoproteins in the $MMR^{-/-}$ mice (Lee et al. 2002). The low-level presence of M6P receptors on macrophages may account for some uptake and effects of phLAL, but the completeness of response was greater than anticipated.

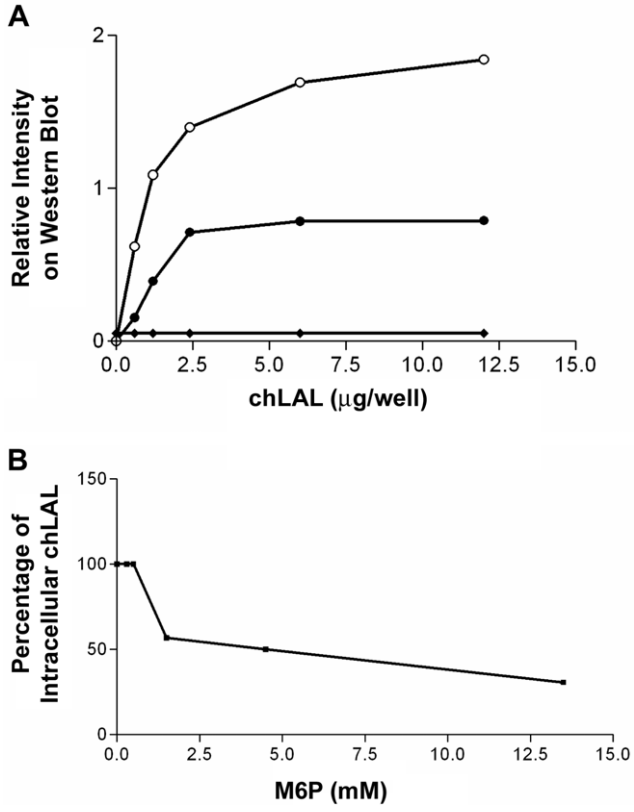

Figure 10 Cellular uptake of chLAL and phLAL in murine macrophages and human fibroblasts. *A,* Western blot analysis of cellular uptake of chLAL and phLAL. Varying amounts of chLAL (*unblackened and blackened circles*) or phLAL (*diamonds*) were placed in media surrounding murine macrophage J774E cells (*unblackened circles*) or human fibroblasts (*blackened circles and diamonds*) for 24 h. After the media was replaced with fresh media without supplemented LAL, the cells were harvested (at 48 h) and were processed for western blot analysis. The intracellular form of hLAL was evaluated by densitometry scanning. Uptake of chLAL occurred in mannose receptor–positive J774E macrophages (*unblackened circles*) and M6P receptor–positive human fibroblasts from an LAL-deficient patient (*blackened circles*). No uptake was observed in human fibroblasts incubated with phLAL (*diamonds*). *B,* Competition of cellular uptake of chLAL in human fibroblasts by M6P. Various amounts of M6P and 12 μg of chLAL were coincubated with human fibroblasts for 24 h. Cells were processed in the same way as described for panel A. The densitometry signal of intracellular hLAL at 0 mM of M6P was defined as 100%. Notice that ~1.5 mM of M6P inhibited ~50% of chLAL uptake in fibroblasts.

The glycoproteins produced by *P. pastoris* have either high-mannose or pauci-mannose structures that contain no galactose and terminal sialic acid residues (fig. 1). In comparison, the CHO cell–produced enzymes, chLAL and agalsidase β (Lee et al. 2003), have glycans that contain terminal sialic acid and uncapped galactose residues that would allow uptake into the lysosomes via the asialoglycoprotein receptor present on hepatocytes (Hudgin et al. 1974; Halberg et al. 1987). Indeed, the CHO cell–produced enzyme agalsidase β has an oligosaccharide content similar to that of chLAL (Lee et al. 2003). Significantly, both agalsidase β and chLAL were deficient in $Man_{7-10}GlcNAc_2$ structures and did not contain $Man_{10-15}GlcNAc_2$ structures. Also, phLAL had little fucosylation, compared with that of chLAL. The majority of phLAL oligosaccharides contained $Man_{8-15}GlcNAc_2$ structures and were similar to those observed in bile salt–stimulated lipase and other proteins produced in *P. pastoris* (Yamada et al. 1994; Kalidas et al. 2001; Hirose et al. 2002; Henriksson et al. 2003). The redistribution of phLAL in the $MMR^{-/-}$ mice could be mediated through the M6P receptor but could also be mediated through other receptors or mechanisms in hepatocytes, such as pinocytosis (Lee et al. 2002). The presence of other mannose receptors with lower affinity for the structures in phLAL cannot be excluded.

The poor distribution of mannosylated BSA to liver and spleen in the $MMR^{-/-}$ mice, along with retention in plasma, supported the MMR as the major controller of plasma levels of mannosylated glycoproteins (Lee et al. 2002). MMR was suggested to play a minor role in

the control of intracellular glycoproteins, particularly lysosomal enzymes; however, measurements were made against a high background of various enzymatic activities, and physiologic roles and specific cellular targeting were not assessed. In contrast, in this case, the physiologic effects of phLAL in the $lal^{-/-};MMR^{-/-}$ background and the delivery of this enzyme to macrophages show that more complex mannosyl structures mediate a different distribution than monomannose-containing glycoproteins. The detection of phLAL in kidney-proximal tubule epithelial cells may well represent reabsorption of filtered hLAL as a result of the prolonged retention of the enzyme in plasma of these mice.

The physiologic effects of phLAL in the $lal^{-/-};MMR^{-/-}$ mice suggest the presence of other uptake mechanisms that can recognize mannosylated oligosaccharides for internalization to the hepatic parenchymal cell lysosome. This was evident by clearance of neutral lipid storage in hepatocytes by phLAL in these mice. Importantly, phLAL was taken up selectively by J774E cells that expressed MMR, whereas no uptake was noted in J774A cells that did not express MMR (Du et al. 2001*b*). Thus, additional receptors in natural macrophages in the liver, spleen, and small intestine could be present for uptake of the highly mannosylated phLAL. M6P receptors are present in liver parenchymal cells and might account for some of the uptake in the absence of MMR (Geuze et al. 1984). However, the lack of uptake of phLAL into human WD fibroblasts, which are positive for M6P receptors and negative for MMR, makes this unlikely (fig. 10C). Additionally, since the phLAL contains longer high-mannose oligosaccharides, the protein could interact with mannose-binding protein in the plasma, leading to subsequent binding of complement factors that stimulate uptake into macrophages as well as hepatocytes and hepatic endothelial cells (Matsuo et al. 1994).

These data demonstrate the physiologic importance of targeting glycoproteins via specific uptake mechanisms for a therapeutic effect on lysosomal storage. These effects are mediated preferentially by MMR, but additional uptake mediated through the M6P receptor and/or endocytosis or pinocytosis may be evident when the MMR is missing or blocked. Such observations may have direct relevance to the treatment of macrophage-storage diseases if the observation of downregulation of MMR in Gaucher storage cells (Boven et al. 2004) is consistent and is shown for other macrophage-storage diseases. Such observations would indicate a redirection to a different population of receptors and/or cells, leading to alternative uptake or differential uptake into various cell types, depending on the expression of MMR at particular stages of the disease process. Clearly, such pathophysiology requires elucidation for the improvement of therapy for patients.

Acknowledgments

We thank Dr. Michel Nussenzweig, a Howard Hughes Medical Institute Investigator at The Rockefeller University, for his generous gift of $MMR^{-/-}$ mice; Bradley Whittaker and Brian Granda at Genzyme, for the carbohydrate analyses; Lisa McMillin, for the histology analysis; Nathan Wenzel, Elizabeth DuPont, Huimin Li, and Lori Stanton, for the technique assistance; and Fannie Anderson, for her clerical support. This work was partially supported by grants from the National Institutes of Health (DK 54930 [to H.D.] and DK36729 [to G.A.G.]) and from the Genzyme Corporation (to G.A.G.).

Web Resources

The URL for data presented herein is as follows:

Online Mendelian Inheritance in Man (OMIM), http://www.ncbi.nlm.gov/Omim/ (for WD and CESD)

References

Anumula KR, Dhume ST (1998) High resolution and high sensitivity methods for oligosaccharide mapping and characterization by normal phase high performance liquid chromatography following derivatization with highly fluorescent anthranilic acid. Glycobiology 8:685–694

Aslanidis C, Ries S, Fehringer P, Buchler C, Klima H, Schmitz G (1996) Genetic and biochemical evidence that CESD and Wolman disease are distinguished by residual lysosomal acid lipase activity. Genomics 33:85–93

Assmann G, Seedorf U (2001) Acid lipase deficiency: Wolman disease and cholesteryl ester storage disease. Vol III. McGraw-Hill Medical Publishing Division, New York

Barton NW, Brady RO, Dambrosia JM, Di Bisceglie AM, Doppelt SH, Hill SC, Mankin HJ, Parker RI, Argoff CE (1991) Replacement therapy for inherited enzyme deficiency—macrophage-targeted glucocerebrosidase for Gaucher's disease. N Engl J Med 324:1464–1470

Beaudet AL, Ferry GD, Nichols BL Jr, Rosenberg HS (1977) Cholesterol ester storage disease: clinical, biochemical, and pathological studies. J Pediatr 90:910–914

Boven LA, van Meurs M, Boot RG, Mehta A, Boon L, Aerts JM, Laman JD (2004) Gaucher cells demonstrate a distinct macrophage phenotype and resemble alternatively activated macrophages. Am J Clin Pathol 122:359–369

Du H, Duanmu M, Witte D, Grabowski GA (1998*a*) Targeted disruption of the mouse lysosomal acid lipase gene: long-term survival with massive cholesteryl ester and triglyceride storage. Hum Mol Genet 7:1347–1354

Du H, Heur M, Duanmu M, Grabowski GA, Hui DY, Witte DP, Mishra J (2001*a*) Lysosomal acid lipase-deficient mice: depletion of white and brown fat, severe hepatosplenomegaly, and shortened life span. J Lipid Res 42:489–500

Du H, Heur M, Witte DP, Ameis D, Grabowski GA (2002) Lysosomal acid lipase deficiency: correction of lipid storage by adenovirus-mediated gene transfer in mice. Hum Gene Ther 13:1361–1372

Du H, Schiavi S, Levine M, Mishra J, Heur M, Grabowski GA (2001*b*) Enzyme therapy for lysosomal acid lipase deficiency in the mouse. Hum Mol Genet 10:1639–1648

Du H, Sheriff S, Bezerra J, Leonova T, Grabowski GA (1998*b*) Molecular and enzymatic analyses of lysosomal acid lipase in cholesteryl ester storage disease. Mol Genet Metab 64: 126–134

Du H, Witte DP, Grabowski GA (1996) Tissue and cellular specific expression of murine lysosomal acid lipase mRNA and protein. J Lipid Res 37:937–949

Folch J, Lees M, Stanley GHS (1957) A simple method for the isolation and purification of total lipids from animal tissues. J Biol Chem 125:497–509

Geuze HJ, Slot JW, Strous GJ, Hasilik A, Von Figura K (1984) Ultrastructural localization of the mannose 6-phosphate receptor in rat liver. J Cell Biol 98:2047–2054

Ginsberg HN, Le NA, Short MP, Ramakrishnan R, Desnick RJ (1987) Suppression of apolipoprotein B production during treatment of cholesteryl ester storage disease with lovastatin: implications for regulation of apolipoprotein B synthesis. J Clin Invest 80:1692–1697

Goldstein JL, Dana SE, Faust JR, Beaudet AL, Brown MS (1975) Role of lysosomal acid lipase in the metabolism of plasma low density lipoprotein: observations in cultured fibroblasts from a patient with cholesteryl ester storage disease. J Biol Chem 250:8487–8495

Grabowski GA, Bove K, Du H (2003) Lysosomal acid lipase deficiencies: Wolman's disease and cholesteryl ester storage disease. In: Walker WA, Goulet OJ, Kleinman RE, Sanderson IR, Sherman PM, Shneider BL (eds) Pediatric gastrointestinal disease: pathophysiology diagnosis management. Brian C. Decker, Hamilton, Ontario

Halberg DF, Wager RE, Farrell DC, Hildreth J 4th, Quesenberry MS, Loeb JA, Holland EC, Drickamer K (1987) Major and minor forms of the rat liver asialoglycoprotein receptor are independent galactose-binding proteins: primary structure and glycosylation heterogeneity of minor receptor forms. J Biol Chem 262:9828–9838

Henriksson H, Denman SE, Campuzano ID, Ademark P, Master ER, Teeri TT, Brumer H 3rd (2003) N-linked glycosylation of native and recombinant cauliflower xyloglucan endotransglycosylase 16A. Biochem J 375:61–73

Hirose M, Kameyama S, Ohi H (2002) Characterization of N-linked oligosaccharides attached to recombinant human antithrombin expressed in the yeast *Pichia pastoris*. Yeast 19:1191–1202

Hudgin RL, Pricer WE Jr, Ashwell G, Stockert RJ, Morell AG (1974) The isolation and properties of a rabbit liver binding protein specific for asialoglycoproteins. J Biol Chem 249: 5536–5543

Kalidas C, Joshi L, Batt C (2001) Characterization of glycosylated variants of β-lactoglobulin expressed in Pichia pastoris. Protein Eng 14:201–207

Krivit W, Peters C, Dusenbery K, Ben-Yoseph Y, Ramsay NK, Wagner JE, Anderson R (2000) Wolman disease successfully treated by bone marrow transplantation. Bone Marrow Transplant 26:567–570

Lee K, Jin X, Zhang K, Copertino L, Andrews L, Baker-Malcolm J, Geagan L, Qiu H, Seiger K, Barngrover D, McPherson JM, Edmunds T (2003) A biochemical and pharmacological comparison of enzyme replacement therapies for the glycolipid storage disorder Fabry disease. Glycobiology 13:305–313

Lee SJ, Evers S, Roeder D, Parlow AF, Risteli J, Risteli L, Lee YC, Feizi T, Langen H, Nussenzweig MC (2002) Mannose receptor-mediated regulation of serum glycoprotein homeostasis. Science 295:1898–1901

Lerouge P, Cabanes-Macheteau M, Rayon C, Fischette-Laine AC, Gomord V, Faye L (1998) N-glycoprotein biosynthesis in plants: recent developments and future trends. Plant Mol Biol 38:31–48

Matsuo H, Funato K, Harashima H, Kiwada H (1994) The complement- but not mannose receptor-mediated phagocytosis is involved in the hepatic uptake of cetylmannoside-modified liposomes in situ. J Drug Target 2:141–146

Meikle PJ, Hopwood JJ, Clague AE, Carey WF (1999) Prevalence of lysosomal storage disorders. JAMA 281:249–254

Montesino R, Garcia R, Quintero O, Cremata JA (1998) Variation in N-linked oligosaccharide structures on heterologous proteins secreted by the methylotrophic yeast *Pichia pastoris*. Protein Expr Purif 14:197–207

Redonnet-Vernhet I, Chatelut M, Basile JP, Salvayre R, Levade T (1997) Cholesteryl ester storage disease: relationship between molecular defects and in situ activity of lysosomal acid lipase. Biochem Mol Med 62:42–49

Rudel LL, Morris MD (1973) Determination of cholesterol using O-phthalaldehyde. J Lipid Res 14:364–366

Sheriff S, Du H, Grabowski GA (1995) Characterization of lysosomal acid lipase by site-directed mutagenesis and heterologous expression. J Biol Chem 270:27766–27772

Trimble RB, Lubowski C, Hauer CR 3rd, Stack R, McNaughton L, Gemmill TR, Kumar SA (2004) Characterization of N- and O-linked glycosylation of recombinant human bile salt–stimulated lipase secreted by *Pichia pastoris*. Glycobiology 14:265–274

Van Dongen JM, Barneveld RA, Geuze HJ, Galjaard H (1984) Immunocytochemistry of lysosomal hydrolases and their precursor forms in normal and mutant human cells. Histochem J 16:941–954

Yamada M, Azuma T, Matsuba T, Iida H, Suzuki H, Yamamoto K, Kohli Y, Hori H (1994) Secretion of human intracellular aspartic proteinase cathepsin E expressed in the methylotrophic yeast, Pichia pastoris and characterization of produced recombinant cathepsin E. Biochim Biophys Acta 1206:279–285